ARTICLES

How Does Benzene in NaY Zeolite Couple to the Framework Vibrations?

Fabien Jousse,*,†,‡ Daniel P. Vercauteren,† and Scott M. Auerbach‡,§

Computational Chemical Physics Group, Institute for Studies in Interface Science, Facultés Universitaires Notre-Dame de la Paix, Rue de Bruxelles 61, B-5000 Namur, Belgium, and Departments of Chemistry and Chemical Engineering, University of Massachusetts, Amherst, Massachusetts 01002

Constrained energy minimization, equilibrium and nonequilibrium molecular dynamics calculations, and constrained Monte Carlo simulations were used to determine the influence of the coupling between benzene adsorbed in a NaY zeolite model (Si/Al = 2) and the framework vibrations on benzene site-to-site dynamics. Benzene at an S_{II} site is strongly coupled to the nearby Na(II) cation, resulting in a decrease of the external vibrational frequency of the center-of-mass of benzene away from this cation by 60 cm^{-1}. Despite this coupling, framework vibrations have remarkably little influence on the site-to-site rate constants of benzene. Although with a fixed framework no dissipation of the excess kinetic energy of the adsorbed molecule can take place and thus no thermalization to equilibrium, energy redistribution from the translational motion of benzene into the internal degrees of freedom of the flexible molecule is seen to provide a good thermalization.

Introduction

Intracrystalline self-diffusion of guest molecules in zeolites[1,2] can be accurately reproduced by kinetic Monte Carlo[3−5] or jump diffusion[6,7] models, as well as lattice gas[8−10] or Ising models.[11] Increasingly, these models are being used to study the long-time transport properties of always more complex and challenging systems with great success and sometimes even predictive potential.[12] Such is the approach applied to the diffusion of benzene in faujasite by Auerbach et al. in a series of recent papers.[4,5,12−18]

At the heart of the kinetic Monte Carlo method (KMC) are both the lattice of sites on which diffusion takes place and the rate constants for the jumps between these sites. Several methods for characterizing the sites and calculating the rates can be employed, from the more approximate to the more accurate.[3,19]

The existence of two types of adsorption sites for benzene in zeolite NaY has been experimentally evidenced[20−30] and confirmed by a number of theoretical calculations,[4,5,31−37] so that this well-established behavior need not be further discussed. In the S_{II} site, the benzene molecule is coordinated to a Na(II) cation in a six-membered ring (6-T), whereas in the shallower W site (W for window), benzene lies in the plane of a 12-T ring between two supercages with its hydrogens coordinated to the oxygens of the framework window; this is claimed to be an effect of "molecular recognition" between the host zeolite frame and the guest molecule.[27,28] Figure 1 presents a view at the atomic level of a supercage of NaY with benzene adsorbed in the two sites: W and S_{II}. It should be noted that the two same sites have been observed, or claimed to be observed, for other

* Corresponding author. E-mail: fjousse@scf.fundp.ac.be.
† Facultés Universitaires Notre-Dame de la Paix.
‡ Department of Chemistry, University of Massachusetts.
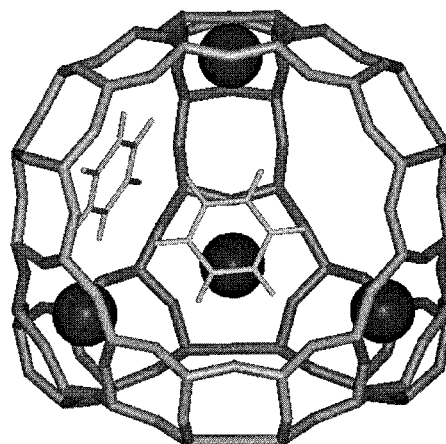§ Department of Chemical Engineering, University of Massachusetts.

Figure 1. View at the atomic level of the two adsorption sites of benzene in zeolite NaY: W (for window) in the 12-T ring window between two supercages and S_{II} near the Na(II) cation schematized by a dark sphere.

faujasitic zeolites such as Na- and CaX,[5,38] HY and USY,[29,39] or H- and NaSAPO-37, and EMT.[30,40,41]

It is much more difficult to determine the rate constants for the jump between the adsorption sites. In their early studies, Auerbach et al. used rates derived from the minimum energy path (MEP) linking two sites, using an Arrhenius dependence with temperature.[4,5,13−15] The prefactors for all rates were set to the usually accepted value of 10^{13} s^{-1}. Since all MEPs exhibit large energy barriers (at least 16 kJ mol^{-1}) and since different MEPs have very different energies, for reasonable temperatures the magnitude of the rates is clearly controlled by the size of the energy part of the diffusion barrier, thus validating this simple model. Although this approach proved quite successful, NMR relaxation measurements of benzene mobility in NaY,

Coupling of Benzene in NaY Zeolite

J. Phys. Chem. B, Vol. 104, No. 37, 2000 **8769**

HY, and USY[29] showed that the difference between prefactors for the $S_{II} \rightarrow S_{II} \rightarrow W$ jumps in HY and USY could reach 3 orders of magnitude, thus shifting partly the control of the magnitude of the rate from the energy to the entropy. This experimental observation motivated the calculation of exact rate constants for the diffusion of benzene in faujasite. In a first paper, devoted to establishing the methods and initiating the actual comparison,[34] we presented rate constants calculated with transition-state theory (TST) and correlation function theory (CFT) for the diffusion of benzene in NaY at infinite dilution. Besides justifying the method of rate calculation for a non-spherical molecule, a number of interesting points resulted from this study. First, we showed that the energetically defavored W site is favored by the explicit inclusion of the entropy. Consequently, the prefactor for the $W \rightarrow S_{II}$ jump becomes 1 order of magnitude smaller than its $S_{II} \rightarrow W$ counterpart. Second, the prefactor for the $W \rightarrow W$ jump is again almost 1 order of magnitude smaller, due to the instability (and therefore high improbability) of the $W \rightarrow W$ path itself. These results clearly justify the application of the methods to the other systems USY or HY, where even larger differences are expected from the experimental observations.[29]

The study presented in ref 34, however, left out two important aspects of the molecular motions that are likely to change the rate constants. Indeed, to reduce the effective number of degrees of freedom to include in the calculation, we neglected both the internal flexibility of the benzene molecule and the motions of the zeolite framework. Since the jumps between sites themselves originate from thermal activation by the framework, we expect the overall effect of the coupling between the framework vibrations, the intramolecular degrees of freedom and the external motions of the benzene molecule to be rather important. Furthermore, the excess kinetic energy of the jumping molecules after the jump can only dissipate in the zeolite frame if framework motions are included. In recent computational studies of benzene in NaY, with a different force field, Mosell et al.[36,37] showed that neglecting the framework vibrations do not change qualitatively, and even quantitatively, the rate constants determined from the potential of mean force. This finding is rather surprising in view of the arguments presented above. Since the rate calculation from the potential of mean force averages all effects, the authors did not present any detail or explanation as to why the framework vibrations have so little effect. Hence, we feel that this issue should be addressed more deeply.

Framework vibrations have been very often neglected in Monte Carlo (MC) or molecular dynamics (MD) studies of sorbate molecules in zeolites. The heat bath provided by the framework has often been replaced by a suitable thermostat in MD simulations. The more direct coupling between the lattice and the sorbed molecules is usually considered of secondary importance. However, it is well-known that some phonon modes of the framework (especially when containing exchangeable cations) are close to the frequency of the external motions of the guest molecules within the zeolite (between 0 and 200 cm^{-1}, for a physically sorbed molecule).[42] It is, therefore, hard to predict in general the effect of the coupling between the molecule and the framework in MD simulations. For systems that do not present large energy barriers between the adsorption sites, such as small alkanes in all-Si zeolites, only a little influence has been observed.[43−46] A recent discussion on this subject can be found in a review article by Demontis and Suffritti.[47]

As already mentioned, transport of benzene in NaY occurs via jumps between the two types of adsorption sites: W and S_{II} (cfr. Figure 1). Therefore, the diffusion of benzene is characterized by the rate constants for the jumps between the sites, that is, $S_{II} \rightarrow S_{II}$, $S_{II} \rightarrow W$, $W \rightarrow S_{II}$, and $W \rightarrow W$. The calculations presented here therefore aim at determining these rates. We used two methods: a harmonic model to estimate the rates from simple energy minimization and equilibrium MD (EMD), and CFT to determine exactly the rates using MC and nonequilibrium MD (NEMD). For both methods, we present a comparison of the results obtained with fixed and flexible frameworks.

In addition to these simulations, we determine the dissipation of the excess translational kinetic energy (TKE) of the adsorbed molecule in its final site after the jump. Indeed, the speed with which this energy dissipates controls the probability for multisite jumps.[48−50] As shown in ref 34, this probability is very small for benzene in NaY, due to the high energy barriers between the sites ($\approx$40 kJ mol^{-1}) as compared to $k_B T$ at the temperature considered (150−500 K). However, since the final reservoir for this energy is the zeolite framework, it is likely that inclusion of framework vibrations will change the speed of the dissipation.

In the next section, we outline the simulation methodology used in this study and the precise improvements made to accommodate flexible or partially flexible framework calculations. The results are presented and discussed in Section III. A short conclusion is given in Section IV.

II. Simulation Methodology

We estimate the rate constants for site-to-site jumps from equilibrium molecular dynamics simulations (EMD) and energy minimizations using a harmonic model and from nonequilibrium molecular dynamics simulations (NEMD) and Monte Carlo (MC) calculations using correlation function theory (CFT). Translational kinetic energy (TKE) dissipation is also determined from EMD and NEMD simulations. The potential energy surface for the intramolecular interactions, the zeolite motions, and the zeolite−guest interactions have been described in previous publications,[4,5] and will not be detailed here. All calculations were performed using a model of zeolite NaY with a Si/Al ratio of 2.0. Long-range Coulombic interactions were computed using the Ewald summation method. The simulation cell consisted of 652 particles, i.e., 640 zeolite atoms and 12 benzene atoms, building a cubic block with a 24.5 Å side, under periodic boundary conditions.

1. Rate Constants from an Harmonic Model. For sufficiently low temperature and sufficiently high energy barriers, the interaction energy between a guest molecule at a stable adsorption site i and the zeolite framework can be approximated by a harmonic potential well. Then, the transition-state theory (TST) rate constant for a jump between this initial site i and a final site f separated by an energy barrier ΔE_{if} takes the form:

$$k_{i \rightarrow f}^{\text{TST}} \approx \nu_{\parallel}^{i} \left(\frac{\prod \nu_{\perp}^{i}}{\prod \nu_{\perp}^{\ddagger}} \right) \times \exp(-\beta \Delta E_{if}) \qquad (1)$$

where $\nu_{\parallel}^{i}$ represents the vibrational frequency of the molecule along the reaction coordinate at the initial site, $\prod \nu_{\perp}$ the product of its vibrations perpendicular to the reaction coordinate, with the superscript i indicating the initial site and the superscript $\ddagger$ the transition state, and $\beta = 1/k_B T$ where k_B is Boltzmann's constant and T the temperature. Supposing that the "perpendicular" vibrations do not change between the initial state i and the transition state, then the site-to-site rate constant takes the following simple form:

$$k_{i \to f}^{\text{TST}} \approx \nu_{\parallel}^{i} \exp(-\beta \Delta E_{if}) \tag{2}$$

where we recognize an Arrhenius law with temperature dependence given by E_{if} and prefactor by $\nu_{\parallel}^{i}$. The vibrational frequencies can be accessed using EMD simulations, by calculating the vibrational density of state (VDOS) of the benzene center-of-mass (CoM). The VDOS is the Fourier Transform of the velocity autocorrelation function (VACF):[51]

$$\text{VACF}(t) = \frac{\langle \mathbf{v}(t) \cdot \mathbf{v}(0) \rangle}{\langle \mathbf{v}(0) \cdot \mathbf{v}(0) \rangle} \tag{3}$$

where **v** is the velocity of the benzene CoM.

Several MD simulations were performed during 200 ps in the microcanonical (N, V, E) ensemble using a fixed time-step of 1 fs. Two runs were initialized from the minimum energy configuration of benzene at an S_{II} site and two others at a W site, either with fixed or with flexible frameworks. The velocities were initialized from a Maxwell–Boltzmann distribution at 600 K, resulting after equilibration of the energy to a temperature close to 300 K.

The energy barrier ΔE_{if} between the initial and final sites can be estimated using constrained energy minimization: the CoM of the benzene molecule is constrained by an external harmonic potential to lie on a plane perpendicular to the axis linking the two minimum energy positions; a number (typically 10) of random insertions and subsequent minimizations are performed to locate the absolute minimum consistent with the constraint. This procedure is repeated at intervals of ≈ 0.2 Å along the axis joining the two sites. Figure 2 presents the benzene minimum energy path (MEP) for an $S_{\text{II}} \to S_{\text{II}}$ jump, determined using this procedure.

In the case of a flexible zeolite framework, it is necessary to fix the position of at least two atoms in the framework, in order to prevent the zeolite to "follow" the guest molecule to its constrained position. Therefore, we fixed the position of 8 silicon atoms of the lattice, chosen near the vertices of the simulation cell. Comparison of the results of the harmonic model between fixed and flexible frameworks allows us to determine exactly the coupling between the guest molecule and the zeolite lattice.

2. Rate Constants from Correlation Function Theory. The CFT rate constants were calculated using the approach formulated by Voter and Doll[52] following a theory presented by Chandler.[53] A detailed description of the methods and of our current implementation can be found in ref 34. In the following, we therefore only briefly outline the method of calculation.

The rate constant for a jump between an initial site i and a final site f is calculated as the product of two terms:

$$k_{i \to f} = k_{i \to f}^{\text{TST}} \times f_{if}(t) \tag{4}$$

where $k_{i \to f}^{\text{TST}}$ is the transition-state theory (TST) rate constant and $f_{if}(t)$ is the so-called dynamical correction factor:

$$k_{i \to f}^{\text{TST}} = \frac{1}{2} \left(\frac{2k_{\text{B}}T}{\pi m} \right)^{1/2} \frac{Q^{\ddagger}}{Q_i} \tag{5}$$

$$f_{if}(t) = \frac{\langle \dot{\zeta}(0) \delta_i[\mathbf{r}(0)] \Theta_f[\mathbf{r}(t)] \rangle}{\langle \dot{\zeta}(0) \delta_i[\mathbf{r}(0)] \Theta_f[\mathbf{r}(\epsilon)] \rangle} \tag{6}$$

In eq 5, $Q^{\ddagger}$ is the partition function of the benzene molecule at the transition state, Q_i is its partition function in the initial state i, k_{B} denotes Boltzmann's constant, T is the temperature, and m is the molecular mass. TST is a static approximation,
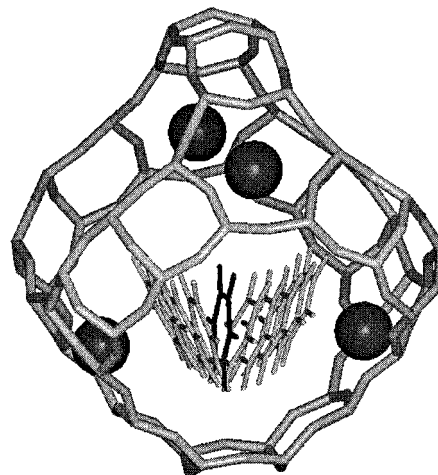

Figure 2. View at the atomic level of the minimum energy path of benzene between two S_{II} sites in zeolite NaY, as determined using constrained energy minimization with a fixed framework. The benzene molecule at the transition state between the two sites is drawn in a darker shade.

assuming that all molecules crossing the dividing surface between the initial and final states in the direction of the final state are reactive.

In eq 6, ζ represents the benzene CoM coordinate perpendicular to the dividing surface bounding state i and $\dot{\zeta}$ its time derivative, $\delta_i[\mathbf{r}]$ represents the Dirac delta function $\delta[\mathbf{r} - \mathbf{r}_i^{\ddagger}]$, and $\Theta_f[\mathbf{r}]$ denotes the standard step function, whose value is 1 if the particle is in final state f and zero otherwise. The denominator of eq 6 represents the equivalent of the TST rate constant of eq 5, cast in CFT form: the TST rate is the flux of molecules crossing the transition state at time 0 that are found in the reactant state after a very short time ϵ. The dynamical correction factor corrects for possible shortcomings of the TST rates by only counting those molecules that are found in the final site after a certain time t.

The TST rate constants $k_{i \to f}^{\text{TST}}$ were evaluated using Voter's displacement vector method.[54] In this method, the ratio of the partition function between two regions of space A and B is computed as

$$\frac{Q_B}{Q_A} = \frac{\langle M_{\beta}[V_B(\mathbf{r} + \mathbf{d}) - V_A(\mathbf{r})] \rangle_A}{\langle M_{\beta}[V_A(\mathbf{r} - \mathbf{d}) - V_B(\mathbf{r})] \rangle_B} \tag{7}$$

where $M_{\beta}(\Delta E) = \min(1, \exp(-\beta \Delta E))$ designs the usual Metropolis sampling function in the canonical ensemble and **d** is a *displacement vector* linking the two regions A and B. The term $\langle M_{\beta}[V_B(\mathbf{r} + \mathbf{d}) - V_A(\mathbf{r})] \rangle_A (\langle M_{\beta}[V_A(\mathbf{r} - \mathbf{d}) - V_B(\mathbf{r})] \rangle_B$, respectively) in eq 7 is simply the MC average over state A (B, respectively) that a fictitious move from A to B (B to A, respectively) with the displacement vector **d** should be accepted.

Equation 7 can be used to determine the ratio of the partition functions $Q^{\ddagger}/Q_i$ of eq 5 by setting

$$\frac{Q^{\ddagger}}{Q_i} = \lim_{\eta \to 0} \frac{Q_B^{\eta}}{Q_A} \tag{8}$$

with

$$V_A(\mathbf{r}) = \begin{cases} V(\mathbf{r}) & \mathbf{r} \in \text{state } i \\ \infty & \mathbf{r} \notin \text{state } i \end{cases} \tag{9}$$

Coupling of Benzene in NaY Zeolite

J. Phys. Chem. B, Vol. 104, No. 37, 2000 **8771**

$$V_B^\eta(\mathbf{r}) = \begin{cases} V(\mathbf{r}) & \mathbf{r} \in [\mathbf{r}^\ddagger - \eta, \mathbf{r}^\ddagger + \eta] \\ \infty & \mathbf{r} \notin [\mathbf{r}^\ddagger - \eta, \mathbf{r}^\ddagger + \eta] \end{cases} \quad (10)$$

where η represents a very small width associated with the transition state, set to 0.2 Å in the practical implementation, and $\mathbf{r}^\ddagger$ denotes the coordinates of the dividing surface.

In ref 34, only 2×10^5 MC steps were needed to determine accurately the TST rates for a rigid molecule and a fixed framework. Accounting for the molecule internal flexibility, however, increases the number of degrees of freedom from 6 to 36, so that it is necessary to perform at least 5×10^5 MC steps in order to get a converged result. Including the motions of all the atoms composing the zeolite framework would lead to a prohibitive computing time. Therefore, and in light of the constrained energy minimization and MD studies reported in the next sections, we limited our TST study of the framework mobility to the sodium cations. Each attempted MC move becomes the combination of a number of moves: the benzene CoM is translated by a random amount, within small limits (typically 0.1 Å); the molecule is rotated, also by a very small amount; if we are to include the internal mobility of the benzene atoms, a number of these atoms are randomly chosen at each step and a translation attempted within very small limits (typically 0.01 Å); and if we include the motion of the sodium cations, some of the cations chosen as mobile are moved. The number of atoms to move, and the maximum allowed displacement for each type of atom, are set depending on the temperature, so that the total acceptance ratio remains close to 0.5. The simulations were typically performed between 150 and 600 K.

Equation 7 can also be used directly to compute the chemical equilibrium constant $\kappa^0(S_{II} \rightarrow W)$ between the two stable adsorption sites. Since there are twice more S_{II} sites than W ones, the chemical equilibrium constant can be defined as

$$\kappa^0(S_{II} \rightarrow W) = \frac{1}{2}\kappa(S_{II} \rightarrow W) = \frac{Q(W)}{Q(S_{II})} \quad (11)$$

The dynamical correction factor of eq 6 can be computed by a canonical average over NEMD runs originating in the transition state.[52,53] The MC sampling in the transition state provides initial molecular positions; the atomic velocities are set according to a Maxwell–Boltzmann distribution at the desired temperature. At a given time t, let us note as $S_f(t)$ the set of the initial N trajectories that are in the final product state. Then the numerator in eq 6 becomes

$$\langle \dot{\zeta}(0)\delta_i[\mathbf{r}(0)]\Theta_f[\mathbf{r}(t)]\rangle = \frac{1}{N}\sum_{i \in S_f(t)} \dot{\zeta}(0) \quad (12)$$

Since TST assumes that all trajectories with initial velocity $\dot{\zeta}(0)$ positive are reactive, the denominator of eq 6 is evaluated as

$$\langle \dot{\zeta}(0)\delta_i[\mathbf{r}(0)]\Theta_f[\mathbf{r}(\epsilon)]\rangle = \frac{1}{N}\sum_{i|\dot{\zeta}(0)>0} \dot{\zeta}(0) \quad (13)$$

The CFT rate constants were calculated for fixed framework and rigid benzene, for fixed framework and flexible benzene, and for flexible benzene and one movable cation (located close to the benzene). In all cases, the dynamical correction factors were computed as the average over 2000 independent NEMD
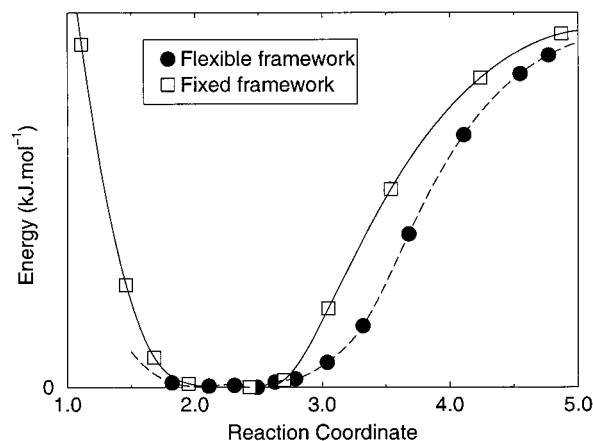

Figure 3. NaY zeolite–benzene interaction energy, as computed from a constrained minimization along the $S_{II} \rightarrow S_{II}$ path, with fixed and flexible framework, using DIZZY[60] with the force field of Auerbach et al.[4] The reaction coordinate is defined as the projection of the benzene center-of-mass onto the $S_{II} \rightarrow S_{II}$ path. Lines are guidelines for the eyes.

runs, each of them lasting only the time necessary to reach a stable state; details of the implementation can be found in ref 34.

3. Kinetic Energy Dissipation. NEMD runs can also be used to follow the dissipation of the excess kinetic energy K of the sorbed molecule after it completed its jump by directly computing the thermal average of $K(t)$ as the molecule thermalizes in the final site. A number of initial conditions for the sorbed molecule near the transition state between two stable sites are prepared, and MD trajectories are run from these initial conditions for a total time of 20 ps, in the microcanonical ensemble with a 1-fs time-step. The starting positions are taken from an MC run constrained next to the transition state, whereas starting velocities are assigned randomly within a Maxwell–Boltzmann distribution at the required temperature. Positioning the molecule next to the transition state between two sites gives an excess initial potential energy that eventually results in an increase of the equilibrium temperature of the system. When all 652 atoms of the zeolite–benzene model are mobile, the temperature increase does not exceed 3 K, whereas when they are fixed, it reaches 120 K. This makes a direct comparison between fixed- and flexible-framework results somewhat more difficult to interpret.

Since 20-ps MD runs with flexible framework require much more computing time than with fixed frame, the thermal averages were computed over only 10 different trajectories. To limit statistical fluctuations, only the temperature of 100 K is presented here. To allow a direct comparison, fixed-framework results are also computed as the average over 10 trajectories initialized at 100 K.

III. Results and Discussion

1. Zeolite–Benzene Coupling at the Initial Site. The NaY–benzene minimum energy path (MEP) were computed with a fixed or flexible framework for both the $S_{II} \rightarrow S_{II}$ and $S_{II} \rightarrow W$ jumps. Figure 3 presents the MEP for the $S_{II} \rightarrow S_{II}$ jump. The reaction coordinate in Figure 3 corresponds to the projection along the $S_{II} \rightarrow S_{II}$ path of the center-of-mass (CoM) of the benzene molecule; its only purpose is to conveniently label the points. Although the flexible-framework MEP, for a given value of the reaction coordinate, is consistently lower than the fixed-framework one, the total energy difference between the maximum and minimum interaction energy seems roughly un-
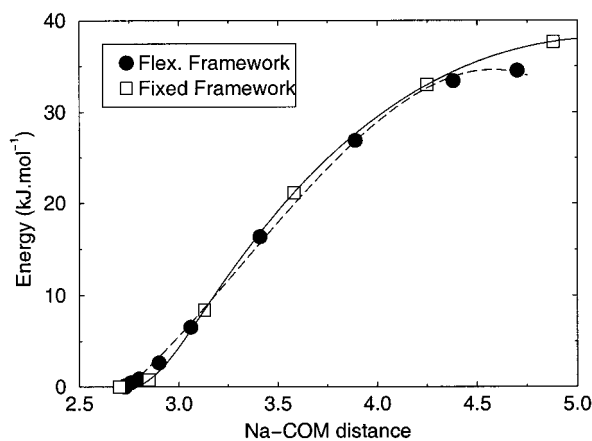
Figure 4. NaY zeolite−benzene interaction energy, as computed from a constrained minimization along the $S_{II} \rightarrow S_{II}$ path, with fixed and flexible framework, using DIZZY[60] with the force field of Auerbach et al.[4] Unlike Figure 3, the reaction coordinate is defined here as the distance between the Na(II) cation in the 6-T ring close to the original S_{II} site and the benzene center-of-mass. Lines are guidelines for the eyes.

changed. Since we did not try to locate precisely the exact transition state on the path, this energy difference should be taken as only indicative of the energy barrier. Still, these first simulations show that the energetic part of the more complete rate constant calculation using a flexible framework is probably not very different of that of the previous fixed-frame computation.[34]

The curvature of the two MEPs near the minimum energy position exhibits a major difference. However, since the "reaction coordinate" is only a label and therefore somewhat artificial, this observation might be misleading. Indeed, in Figure 4 we also present the NaY−benzene interaction energy along the MEP but plotted against the distance between the Na(II) cation in the 6-T ring and the CoM of the benzene molecule. With this choice of axis, the fixed and flexible lattice curves overlap almost exactly, except for the highest energy point. At the S_{II} site, the interaction energy mostly originates from the interaction between the cation and the benzene. The curves in Figure 3 reflect that the Na(II) cation "follows" the benzene molecule as it moves away. This suggests that the coupling between the cation and the external motions of benzene might be important. Indeed, the external vibrations of the benzene CoM in NaY at the S_{II} site were found to lie between 20 and 100 cm^{-1}.[34] The frequency of the translational motions of a Na$^+$ cation in an S_{II} site is between 100 and 200 cm^{-1}, according to far-IR experiments and simulations.[55] Therefore, a large coupling is expected to show up. On the other hand, the rest of the NaY frame seems not to have a large influence, which suggests that the coupling might be accurately reproduced by considering the motions of the Na(II) cation alone.

The MEP for the $S_{II} \rightarrow W$ jump leads to the same conclusion as for the $S_{II} \rightarrow S_{II}$ one: the energy barrier with the flexible NaY framework is very slightly lower than in the fixed-framework case (3 kJ mol^{-1} at the most), but the position of the transition state appears to be unchanged.

As we have seen in Section II, relatively short molecular dynamics (MD) simulations of about 200 ps at 300 K can be used to extract the frequencies of the external motions of benzene at a given site of the zeolite, whereas computing the self-diffusion coefficient for this system would require a prohibitive amount of computing time. The benzene frequencies are very sensitive to the coupling between the guest molecular motions and both the zeolite phonons and the motions of the
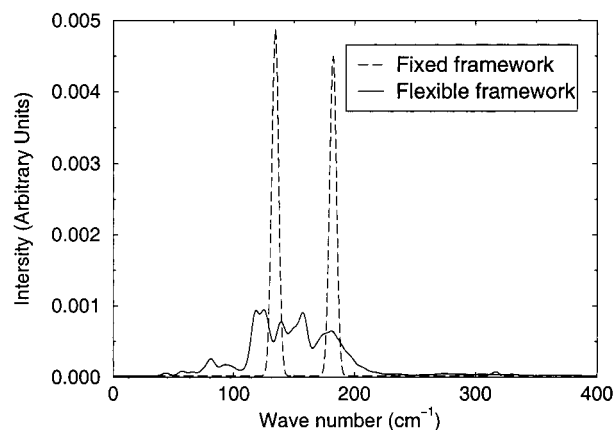

Figure 5. Low-frequency vibrational density of states of the cation Na605 of zeolite NaY in the absence of any sorbed molecule, calculated from a 200-ps MD run at 300 K, using the DIZZY code[60] with the force field of Auerbach et al.[4]
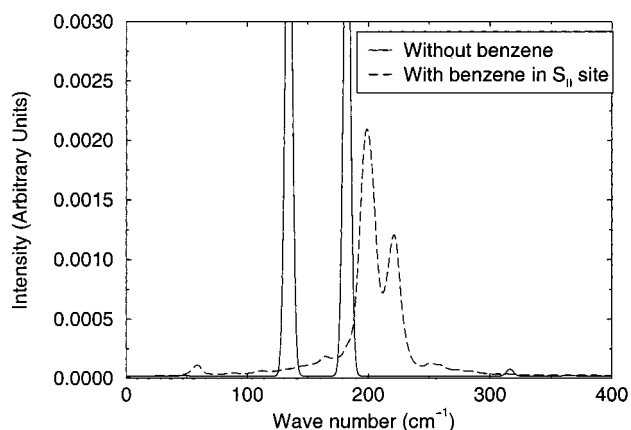

Figure 6. Low-frequency vibrational density of states of the cation Na605 of zeolite NaY when only this ion is allowed to move, calculated from a 200-ps MD run at 300 K using the DIZZY code[60] and the force field of Auerbach et al.[4]

sodium cations. Since the coupling is expected to be strongest between the benzene molecule at an S_{II} site and the nearby Na(II) cation (noted afterwards as Na605, corresponding to its numbering in the zeolite model), we focus on the vibrational density of states (VDOS) of this Na605 ion and of the COM of the benzene molecule calculated: (i) with fixed framework, (ii) with only the Na605 ion (and the sorbed molecule) moving, and (iii) with a full flexible framework.

Figure 5 presents the low-frequency VDOS of the Na605 ion in the bare zeolite (i.e., without benzene) in the cases this ion is embedded in a fixed and fully flexible framework. When only this ion is allowed to relax, its VDOS is made up of two distinct delta-peaks at 145 and 180 cm^{-1}, which can be considered as the "natural" vibrational frequencies of the Na(II) ion at an S_{II} site. Coupling with the framework phonons is seen to complicate the spectrum: instead of two well-separated peaks, we observe a complex mountain chain stretching approximately between 100 and 200 cm^{-1}. This frequency range is in good agreement with experimental and other theoretical data.[55] It is therefore much simpler, in a first step, to analyze the coupling between the Na$^+$ cation in the 6-T ring and the benzene molecule at the S_{II} site in the case where only one ion is allowed to relax. We begin this analysis with Figure 6, where we compare the VDOS of the Na605 cation with and without adsorbed benzene. One sees clearly that the vibrational frequencies of this cation are strongly affected by the presence of the benzene molecule at
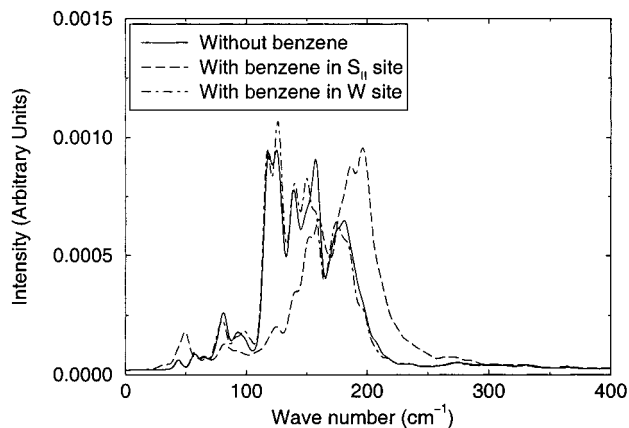
Figure 7. Low-frequency vibrational density of states of the cation Na605 of zeolite NaY when the complete framework is allowed to move, calculated from a 200-ps MD run at 300 K using the DIZZY code[60] and the force field of Auerbach et al.[4]
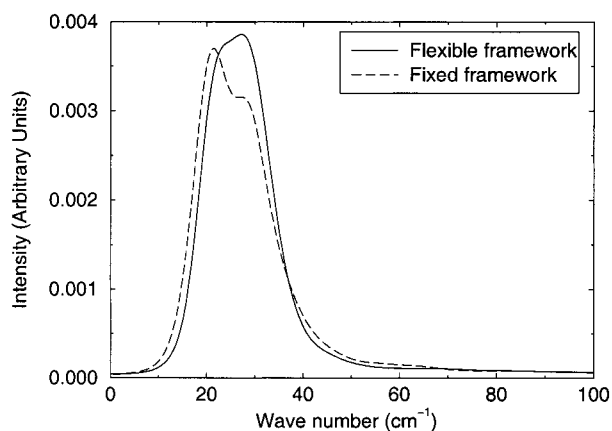

Figure 8. Low-frequency vibrational density of states of the center-of-mass of benzene at a W site of zeolite NaY, calculated from a 200-ps MD run at 300 K using the DIZZY code[60] and the force field of Auerbach et al.[4]

an S_{II} site, shifting them more than 50 cm^{-1} toward higher wavenumbers. A general broadening of the bands due to the coupling can also be observed. The same observations can be made when the complete flexibility of the NaY framework is included, as shown in Figure 7. Clearly, we observe the same upward shift of the Na(II) vibrational frequencies upon adsorption of benzene as in Figure 6. Figure 7 also presents the VDOS of the Na605 cation when benzene is adsorbed in the nearest W site. In this case, no shift is observed, showing the absence of coupling between this Na$^+$ cation and the sorbed molecule in a W site.

The VDOS of the benzene CoM when benzene is located at a W or S_{II} site of NaY is presented in Figures 8 and 9, respectively, for both fixed and flexible frameworks. Figure 9 also displays the VDOS of benzene when all the framework atoms but the Na605 cation are kept fixed.

The VDOS of the benzene CoM in NaY has already been described in ref 34 in the fixed-framework case. In the W site, we observe only two broad bands at low frequency (LF), $\approx$22 and 32 cm^{-1}, whereas in the S_{II} site, a double band at very LF, $\approx$15 cm^{-1}, is followed by a high-frequency (HF) peak at $\approx$90 cm^{-1}. This last peak is attributed to the vibration of the molecule away from the cation and hence cannot be found in the W site of NaY.

One sees in Figure 8 that going from a fixed to a flexible framework does not change significantly the vibrations of benzene CoM in the W site. This means that the coupling
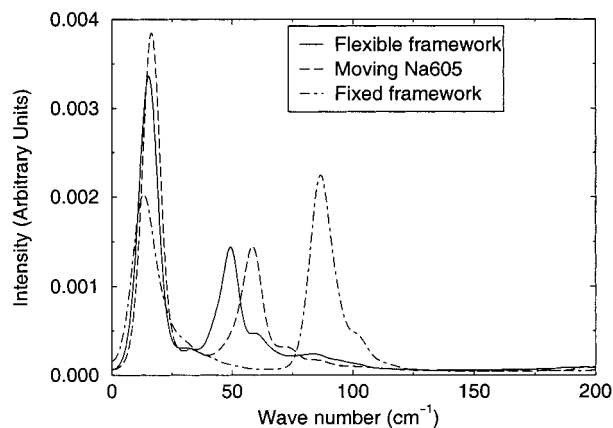

Figure 9. Low-frequency vibrational density of states of the center-of-mass of benzene at an S_{II} site of zeolite NaY, calculated from a 200-ps MD run at 300 K using the DIZZY code[60] and the force field of Auerbach et al.[4]

between the host framework and the guest molecule does not affect the vibrations of the benzene CoM, which sits on a high symmetry axis. This observation in turn suggests that the most probable coupling will occur between the window breathing mode of the zeolite and the ring-opening mode of the benzene molecule.

On the other hand, inclusion of the framework vibrations completely changes the motions of benzene at the S_{II} site, as can be seen in Figure 9. Whereas the LF peak remains roughly unaffected, the HF peak shifts from $\approx$90 cm^{-1} for a fixed framework to $\approx$60 cm^{-1} when the motions of the Na605 cation are included and further down to $\approx$50 cm^{-1} for a fully flexible framework. This denotes a strong coupling between the vibration of the Na605 cation and the motion "away from the cation" of the benzene CoM. This strong coupling has been noted already in Figure 6, which displays the VDOS of this Na605 cation. The upward shift of the vibrational frequency of this cation is counterbalanced by the strong downward shift of the benzene CoM vibration. We now can also discuss the small peak at $\approx$50 cm^{-1} in Figure 6, indicating the mixing of the vibrational frequencies of the Na605 cation and of the benzene CoM. Most of the coupling seems to come from the Na605 cation. In this light, the further 10 cm^{-1} shift that is observed when a fully flexible framework is considered is more probably due to the change of the vibrational frequencies of the Na605 cation, as a consequence of its interaction with the rest of the zeolite framework rather than by any direct coupling between benzene and the zeolite. A comparison between the calculated benzene CoM frequencies and the LF spectrum of the H atoms in benzene adsorbed on NaY measured by inelastic neutron spectroscopy[56] shows that the computed frequencies are too high when framework motions are left out of the calculation. The decrease due to the coupling makes the frequencies of these vibrations more comparable to the experimental ones.

The above observations demonstrate the existence of a strong coupling between the vibrations of the benzene CoM at an S_{II} site with the Na(II) cation located in the neighboring 6-T ring. There is, however, no evidence of a coupling between the motions of the benzene CoM at a W site and the framework. Furthermore, the frequency shift of the HF motion of the benzene CoM at an S_{II} site is almost identical when only the coupling with the Na(II) cation is considered or when the whole flexible framework is included, the difference being attributable to the secondary coupling between the cation and the framework. Therefore, it is expected that the inclusion of the framework
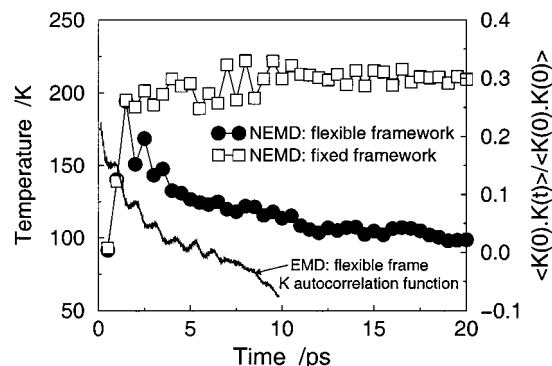
Figure 10. Average total kinetic energy of a benzene molecule starting at time $t = 0$ with a kinetic energy corresponding to 100 K next to the transition state between two stable NaY S_{II} sites, computed as the average over 10 NEMD trajectories using the DIZZY code[60] with the force field of Auerbach et al.,[4] with either a fixed or flexible framework, and autocorrelation function of the total kinetic energy of benzene, calculated during a single equilibrium MD run in a stable S_{II} site, with a flexible framework.

Figure 11. Average translational kinetic energy of a benzene molecule starting at time $t = 0$ with a kinetic energy corresponding to 100 K next to the transition state between two stable NaY S_{II} sites, computed as the average over 10 NEMD trajectories using the DIZZY code[60] with the force field of Auerbach et al.,[4] with either a fixed or flexible framework.

motions will mainly, if not uniquely, affect the benzene CoM motions at the S_{II} site, but not at the W site, through coupling with the motions of the Na(II) cation.

In the harmonic approximation, the transition-state theory (TST) rate constants are proportional to the frequency of the motion of benzene along the reaction coordinate between the zeolite sites. Therefore, we expect that inclusion of the framework vibrations will significantly change the TST pre-factors for all jumps leaving an S_{II} site but will not affect the jumps out of a W site. Since the vibration frequency at the S_{II} site *decreases*, the effect should be an entropic favoring of the S_{II} site. We will see in the Section III.3 that this is *not* the case.

2. Kinetic Energy Dissipation. A benzene molecule jumping over the energy barrier between two zeolite sites gains an excess translational kinetic energy (KE) as it falls down the barrier into the final site. This excess energy then dissipates, and the molecule thermalizes in the final site. Note that it is the *translational* KE of the benzene CoM rather than the total KE that allows the jump. We can distinguish in general three processes contributing to the energy dissipation, that is, redistribution of the excess KE into (i) the zeolitic framework; (ii) other sorbed molecules; and (iii) the molecule's internal degrees of freedom. Whereas the first two processes have already been studied in the case of spherical Lennard-Jones adsorbates in zeolites,[45,57] the influence of redistribution of the energy into the internal vibrational modes of the guest molecule has not been studied yet, to the best of our knowledge. Therefore, we focus on this process by considering only infinite dilution. Figure 10 presents the evolution of the total KE of a benzene molecule, computed as the average over 20 NEMD runs initialized close to the transition state, both with fixed and flexible frameworks, at the temperature of 100 K. In both cases, the total KE initially increases strongly, as the molecule falls down the energy barrier; the oscillating behavior afterwards represents the alternate shift of the total energy between potential and kinetic components. With flexible frame, the KE then decreases exponentially down to the equilibrium temperature, with a time constant of ≈5 ps. Since our simulations are per-formed with only one benzene molecule, no exchange with other molecules can take place, and the dissipation is therefore exclu-sively due to the exchange with the zeolite framework, which acts as a thermal bath. When the framework is held rigid, no dissipation is observed and the KE stabilizes at a higher value.

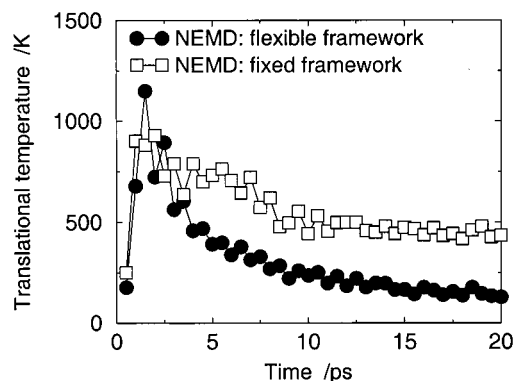Linear response theory and the fluctuation−dissipation

theorem state that the return to equilibrium of any quantity A is proportional to its equilibrium fluctuations:[58,59] $\tilde{A}(t) \propto \langle A(0) \cdot A(t) \rangle$. In Figure 10, we also present the autocorrelation function of the benzene total KE during a 20-ps equilibrium MD run at a stable S_{II} site. This autocorrelation function, indeed, presents the same behavior as the direct measure of the energy dissipa-tion, with a similar time constant.

Figure 11 presents the translational KE of a benzene molecule during the same NEMD runs as in Figure 10. With flexible framework, we observe the same behavior as in Figure 10, that is, sharp initial increase followed by energy dissipation with a time constant of ≈5 ps. With fixed framework, however, the KE behaves differently: indeed, we now have the same type of energy dissipation as for the flexible framework, with an identical time constant of ≈5 ps. This dissipation is due to the redistribution of the translational KE of benzene into its internal degrees of freedom. That this redistribution has the same time constant as the energy dissipation into the framework shows that they probably have the same cause: collisions between the guest molecule and the framework, which speeds up energy redistribution.

It is clear that the energy dissipation of benzene in its final site after a jump is quite different when framework vibrations are included. The site-to-site dynamics of benzene, however, depends mainly on the translational KE. This translational energy dissipates by redistribution into the internal degrees of freedom of the flexible benzene molecule with the correct time constant, even when framework vibrations are not included. This suggests that NEMD runs with fixed framework capture correctly the site-to-site dynamics of benzene adsorbed in NaY. Indeed, it was shown in ref 34 that the dynamical correction factor to the equilibrium constant reaches a plateau in less than 2 ps. In this short time, the total temperature difference between fixed and flexible framework cases has not reached the catastrophic value it takes after the system returns to equilibrium. Note that the conclusion reached here might not hold for an atomic adsorbate.

3. Guest Molecule Jump Rates. The rate constants and chemical equilibrium constants presented in ref 34 were calculated not only with a fixed framework but also for a rigid benzene molecule. The influence of the benzene internal flexibility on the chemical equilibrium constants and on the jump rates will be discussed in this section, together with the influence of the framework vibrations.

The MD study presented in the previous section has shown that the coupling between benzene and the NaY zeolite
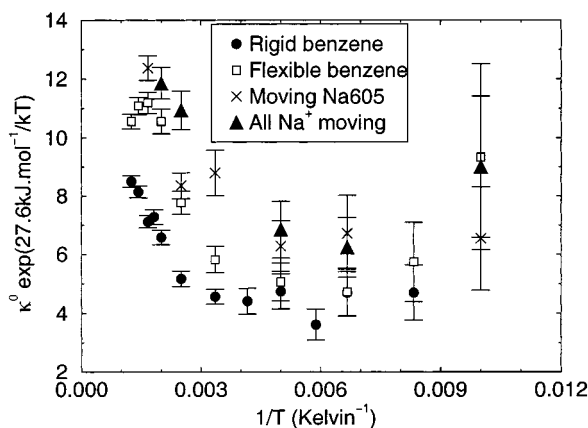
Coupling of Benzene in NaY Zeolite

J. Phys. Chem. B, Vol. 104, No. 37, 2000 **8775**

Figure 12. Chemical equilibrium constant of benzene between S_{II} and W sites of NaY, compensated for the apparent Arrhenius behavior: $\kappa^0(S_{II} \rightarrow W) \times \exp(27.6\ \text{kJ mol}^{-1}/k_B T)$, calculated using Voter's displacement vector method implemented within the DIZZY code[60] and the force field of Auerbach et al.:[4] filled circles, rigid benzene, fixed framework; open squares, flexible benzene, fixed framework; crosses, flexible benzene, fixed framework except for the Na605 cation; filled triangles, flexible benzene, all cations are allowed to move.

framework originates mostly from the coupling with the Na(II) cation. The first approximation to a flexible framework rate constant calculation is naturally to include only the motions of the particular Na$^+$ cation next to the S_{II} site we are exploring. In a second approximation, we considered the motion of all Na$^+$ cations in the zeolite.

The chemical equilibrium constants are calculated directly in one run using Voter's displacement vector method,[54] whereas the rate constants require the additional computation of the dynamical correction factor.[34,52] In the next subsection, we first analyze the effects of the benzene and zeolite flexibility on the chemical equilibrium constants.

Figure 12 presents the chemical equilibrium constants calculated from Voter's displacement vector method in four cases: rigid benzene and fixed zeolite framework (filled circles); flexible benzene and fixed framework (open squares); flexible benzene with movable Na605 cation (crosses); and flexible benzene with all Na$^+$ cation movable (filled triangles). κ^0 in Figure 12 has been multiplied by $\exp(27.6\ \text{kJ mol} - 1/kT)$ to compensate for the apparent Arrhenius behavior of the chemical equilibrium constant in the fixed framework/rigid benzene case (see Figure 6 of ref 34 for a more complete picture). Note that the error bars grow larger as the number of degrees of freedom considered in the calculation increases, reflecting the larger statistical uncertainties. The error bars are particularly important at low temperature, due to the smaller fraction of attempted displacements that actually contribute to the total average in the Voter's displacement vector method.

The dependence with temperature of κ^0 has already been discussed for the fixed NaY zeolite/rigid benzene calculation in ref 34: an Arrhenius behavior over the whole range of temperatures was observed, with an activation energy of ≈ 28 kJ mol^{-1}. When the data are compensated for this Arrhenius behavior, as in Figure 12, we observe finer details of the temperature dependence. At low temperature, the preexponential factor is roughly constant and equals ≈ 4 to 5, showing that the W site is entropically favored as compared to the S_{II} site. As the temperature increases so does κ^0, reaching ≈ 9 at 600 K, showing that the W site is more and more favored with respect to the S_{II} site. The origin of this favoring is probably to be found in the smaller vibrational frequency of the benzene CoM at the W site.

Including the benzene internal flexibility in the calculation does not change qualitatively the picture obtained with a rigid molecule. There is no apparent change in the activation energy. At low temperature, the prefactor does not show any statistically significant deviation from the rigid benzene case. Only at high temperature do we observe a deviation, as the favoring of the W site noted before is enhanced by the internal vibrations of the benzene molecule. In the simplest harmonic approximation to the molecular entropy, the partition function is proportional to the product of the inverse of the molecule harmonic frequencies. Since there is not likely to be any coupling between the benzene internal vibrational modes and the Na(II) cation, due to the large difference in the frequencies, the larger favoring when molecular flexibility is included then means that the internal modes of benzene have a higher frequency at the S_{II} site than at the W one. Indeed, benzene at the S_{II} site is slightly bent, so that the corresponding frequencies are tightened, as compared to the W site where the symmetry retains the shape of the free benzene molecule.

Crosses in Figure 12 correspond to the results of the calculation when the motions of the Na605 cation (i.e., close to the benzene molecule in the S_{II} site) are accounted for. The curve built from these crosses seems slightly shifted by one or two units along the vertical axis, as compared to the curve representing the simulation with flexible benzene but fixed Na605 cation (open squares). This shift represents again an entropic favoring of the W site as compared to the S_{II} site. This contradicts the trends observed in the molecular dynamics simulations presented in Section III.1. Indeed, the benzene CoM vibration becomes sloppier when the cation motions are included, thus suggesting that the κ^0 would decrease. The opposite observation indicates that the simple harmonic model fails to give an adequate behavior of benzene at an S_{II} site. Indeed, the conclusion drawn from the MD data was based on observing the motions of the benzene center-of-mass only; we have noted in section III.1, however, that in the constrained minimization the Na$^+$ cation follows the benzene molecule during its jump. Thus, the adequate system to consider, rather than the benzene molecule alone, is the complex formed by this cation and the molecule; at the W site, it would consist of the "free" molecule at the W site on one hand, and the uncoupled Na(II) cation on the other. The harmonic model in this case suggests that the chemical equilibrium constant should be in fact *unchanged* whether the cation motions are included or not. Indeed, the chemical equilibrium constant calculation shows, rather than the expected decrease of κ^0 by a factor of 2, a slight increase of approximately one unit. This observation really shows that the meaningful reaction coordinate in the case of an $S_{II} \rightarrow W$ jump involves both the benzene molecule *and* the Na(II) cation.

As was expected from Section III.1, including the motion of the other cations in the simulation does not change the chemical equilibrium constant.

The jump rate constants were computed in two steps: a transition-state theory-like calculation using Voter's displacement vector method and a dynamical correction factor calculation with our personal implementation of Chandler's ideas. In general, an Arrhenius behavior was noted over the whole range of temperatures studied, that is, 150−600 K. An example of the temperature dependence of the rate constants can be found in Figure 9 of ref 34. Only rates for the $S_{II} \rightarrow S_{II}$, $S_{II} \rightarrow W$, and $W \rightarrow S_{II}$ jumps were computed with flexible benzene and movable cations: indeed, it was found in ref 34 that the $W \rightarrow W$ path is very unstable and thus requires very long calculations

TABLE 1: Activation Energies and Arrhenius Prefactors of the Rate Constants for the Jumps Between S_{II} and W Sites of Benzene in Zeolite NaY, Calculated Using the Correlation Function Procedure

	activation energy (kJ mol^{-1})			Arrhenius prefactors (s^{-1})		
	$S_{II} \rightarrow S_{II}$	$S_{II} \rightarrow W$	$W \rightarrow S_{II}$	$S_{II} \rightarrow S_{II}$	$S_{II} \rightarrow W$	$W \rightarrow S_{II}$
rigid benzene/fixed framework	36.8 ± 0.3	44.4 ± 0.1	16.4 ± 0.3	0.83×10^{13}	0.80×10^{13}	1.06×10^{12}
flexible benzene/fixed framework	36.5 ± 0.4	44.2 ± 0.4	15.9 ± 0.3	1.15×10^{13}	1.38×10^{13}	1.13×10^{12}
flexible benzene/movable Na605	35.8 ± 0.7	42.6 ± 0.3	14.6 ± 0.5	1.25×10^{13}	0.70×10^{13}	0.64×10^{12}

to be estimated; therefore, considering additional degrees of freedom would lead to a prohibitive computing time.

Table 1 summarizes the activation energies and prefactors calculated from a linear fit of ln k as a function of $1/T$, for fixed benzene and rigid zeolite framework, flexible benzene with rigid framework, and flexible benzene and movable Na605 cation. In the case of the $S_{II} \rightarrow W$ jump, we also included a study with all Na$^+$ ions allowed to relax. The simulations presented in the previous sections suggested that the effect of these additional degrees of freedom would probably be negligible, except in computing time, and therefore these calculations were not performed for all jumps. Note that the activation energies come with error bars that reflect the uncertainties of the linear regression; these error bars therefore assume true Arrhenius behavior over the whole range of temperature. A slight deviation from true Arrhenius behavior results in slightly larger error bars but also in much larger uncertainties on the prefactors. Therefore, the prefactors given in Table 1 are more indicative of an order of magnitude, rather than of an exact value.

Including the benzene internal mobility in the rate constant calculations results in a slight lowering of the activation energies for all the jumps considered. This lowering, however, is statistically insignificant, since the error bars overlap in all cases. The order of magnitude of the prefactors clearly does not change. We note an increase of the prefactors with temperature for both the $S_{II} \rightarrow S_{II}$ and $S_{II} \rightarrow W$ jumps, in accordance with the chemical equilibrium constant calculations.

Including the motions of the Na605 cation close to the benzene molecule at an S_{II} site does not change significantly the activation energy for the $S_{II} \rightarrow S_{II}$ jump. On the other hand, there is a slight but significant lowering (about 1.5 kJ mol^{-1}) of both the $S_{II} \rightarrow W$ and the $W \rightarrow S_{II}$ activation energies. That the change in the energetics of the guest dynamics is so small is consistent with the MEP calculations presented in Section III.1. The order of magnitude of the prefactors again does not change. However, while there is clearly no influence on the $S_{II} \rightarrow S_{II}$ rate constant, we note a decrease of both the $S_{II} \rightarrow W$ and $W \rightarrow S_{II}$ prefactors. That the $S_{II} \rightarrow S_{II}$ rate remains unaffected by the inclusion of the Na605 motions indicates that the transition state between two sites is affected in the same way as the S_{II} site itself; the decrease of both $W \rightarrow S_{II}$ and $S_{II} \rightarrow W$ activation energies and prefactors indicates that in this case, the influence of the Na605 motions is different at the transition state and at the stable sites. It was found in ref 34 that both $S_{II} \rightarrow W$ and $S_{II} \rightarrow S_{II}$ jumps presented the same prefactors; this finding agreed with the harmonic model, where the prefactors are controlled by the same vibration "away from the cation" of the benzene CoM, if the perpendicular vibrations are the same at both transition states. Including the vibration of the Na605 cation lifts the equivalence between the two transition states.

We did not perform the complete correlation function computations with all Na$^+$ cations moving but limited ourselves to the TST calculations; these, indeed, have been shown to give a good first approximation to the exact (i.e., correlation function theory) rate constants[34] for benzene in NaY. In all cases studied,

inclusion of the motions of all ions did not change significantly either the activation energy or the prefactors of the transition-state theory rates. This is consistent with what was observed for the chemical equilibrium constants and demonstrates the small effect of the other cations on the benzene molecule both at the stable sites and at the transition states.

IV. Conclusion

The diffusion of benzene in zeolite NaY occurs via activated hops between the two types of stable adsorption sites, noted S_{II} and W. In a previous study,[34] we computed exact rate constants for the jumps of benzene in a NaY zeolite model (Si/Al = 2) but without accounting either for the internal flexibility of the benzene molecule or of the zeolite framework. In the present paper, we have performed atomistic simulations on benzene sorbed in the same NaY zeolite model, in order determine and explain the influence of these two types of motions on the dynamics of the guest molecule.

Constrained energy minimizations using the DIZZY code with the forcefield of Auerbach et al.[4] were used to determine the minimum energy path (MEP) between two sites, both for a fixed and flexible zeolite framework. The energy barriers for both the $S_{II} \rightarrow S_{II}$ and $S_{II} \rightarrow W$ jumps were hardly affected by the framework mobility. A large coupling appears between the Na(II) cation located in the 6-T ring near the benzene molecule at an S_{II} site and the benzene itself.

Nonequilibrium molecular dynamics (EMD) simulations initiated with the benzene molecule at a given site were performed to extract the frequencies of the motions of the benzene center-of-mass (CoM), both with fixed and flexible frameworks; in the harmonic model, the Arrhenius prefactor of the jump rates is directly proportional to the frequency of the motion along the reaction coordinate. These studies confirm the very large coupling between the Na(II) cation and the benzene molecule at an S_{II} site, as the frequencies of the cation and of the benzene CoM motions are shifted by 50 cm^{-1} toward higher and smaller wavenumbers, respectively. The mobility of the rest of the framework, however, does not greatly influence the motions of benzene at the S_{II} site. In the W site, it seems that there are no differences between the external motions of the benzene molecule with a fixed or flexible framework. These observations suggest that it is necessary to include the motion of the Na(II) cation in order to achieve an accurate description of the jump rates involving benzene at an S_{II} site. They also suggest that the coupling between the benzene molecule and the rest of the framework is of secondary importance.

The energy dissipation of benzene in the final site after it completed its jump was studied by a direct monitoring of the kinetic energy (KE) of benzene during NEMD simulations that were started next to the transition state between two sites. The total KE dissipates exponentially into the framework with a time constant of ≈5 ps. When framework vibrations are left out of the calculation, no dissipation of the total KE can take place. However, the translational KE is seen to redistribute into the internal vibrations of the benzene molecule, with the same 5-ps rate constant whether the framework is fixed or flexible. Since

Coupling of Benzene in NaY Zeolite

J. Phys. Chem. B, Vol. 104, No. 37, 2000 **8777**

it is the translational KE that governs site-to-site jumps, we expect that MD simulations with a fixed framework will give adequate site-to-site dynamics.

Finally, transition-state theory (TST) and correlation function theory (CFT) calculations were performed using the methodology established in ref 34, to determine the chemical equilibrium constant $\kappa^0(S_{II} \rightarrow W)$ between the two stable adsorption sites and the corresponding jump rates $k(S_{II} \rightarrow S_{II})$, $k(S_{II} \rightarrow W)$, and $k(W \rightarrow S_{II})$. Due to the increase in computing time for the Monte Carlo simulations with the increasing number of degrees of freedom, the rates and chemical equilibrium constants were not calculated with complete flexibility of the framework, but were limited to 4 cases: with a fixed framework and a rigid benzene molecule; with a fixed framework and a flexible benzene molecule; with a flexible benzene and one mobile Na(II) cation next to the benzene's S_{II} site; and with a flexible benzene and all Na$^+$ cations movable. Accounting for the flexibility of the benzene molecule changes significantly the chemical equilibrium constant: the W site, which is entropically favored over the S_{II} site even for a rigid benzene calculation, becomes even more favored, due to the tightening of the intramolecular vibrations at the S_{II} site. The effect on the jump rates is similar but remains small, and the order of magnitude of the prefactors is not perturbed. The activation energies also remain unchanged. Including the vibration of the Na(II) cation again seems to favor the W site over the S_{II} one. This observation contradicts the trends deduced from the MD simulation using the simple harmonic model, since the vibration of the benzene molecule at an S_{II} site corresponding to the motion toward a W site was seen to *decrease* significantly. This shows that the harmonic model in its simplest form is not applicable in this case and that the effective reaction coordinate involves both the Na(II) cation and the benzene molecule.

Inclusion of the benzene flexibility and the motions of the Na$^+$ cation has a surprisingly small final effect on the rate constants, in spite of a very large coupling between the benzene molecule at an S_{II} site and the Na$^+$ cation in the nearby 6-T ring. Indeed, the activation energies are barely affected, and even the Arrhenius prefactors are very close to their rigid benzene molecule/fixed framework values. This result is in good accordance with the findings of Mosell et al.[36,37] MD simulations show that the general coupling between a benzene molecule and the zeolite framework is small, except for benzene at an S_{II} site and the Na(II) cation in the nearby 6-T ring. The dynamics of all the other Na$^+$ cations have no clear influence: the coupling is strongly local. It is clear that, although the final rate constants are close to the rigid framework ones, the dynamics of the benzene molecule at the S_{II} site is profoundly affected by the dynamics of the Na$^+$ cation. That the final hopping rates are almost unaffected appears as a *fortuitous* result of the particular coupling that is observed in this case and cannot be generalized to other molecule–cation–zeolite systems. The CFT rate constants have to be calculated in order to determine the exact influence; indeed, MD simulations with the harmonic model would have suggested an influence opposite of what is observed.

The results presented in this article do not change the conclusions of ref 34. The rigid benzene/fixed zeolite framework approach is seen to give results very close to the more complete flexible benzene/mobile cations system. This finding cannot be generalized to other systems. In a first approximation, only the dynamics of the Na$^+$ cations close to the guest molecule needs to be included. We did not investigate directly the influence of the local zeolite modes on the final rates, but the MD simulations suggest that it would be small.

References and Notes

(1) Kärger, J. *Phys. Rev. A* **1992**, *45*, 4173.
(2) Chen, N. Y.; Degnan, T. F.; Smith, C. M. *Molecular Transport and Reaction in Zeolites*; VCH Publishers: New York, 1994.
(3) June, R. L.; Bell, A. T.; Theodorou, D. N. *J. Phys. Chem.* **1991**, *95*, 8866.
(4) Auerbach, S. M.; Henson, N. J.; Cheetham, A. K.; Metiu, H. I. *J. Phys. Chem.* **1995**, *99*, 10600.
(5) Auerbach, S. M.; Bull, L. M.; Henson, N. J.; Metiu, H. I.; Cheetham, A. K. *J. Phys. Chem.* **1996**, *100*, 5923.
(6) Jousse, F.; Leherte, L.; Vercauteren, D. P. *J. Phys. Chem. B* **1997**, *101*, 4717.
(7) Jousse, F.; Auerbach, S. M.; Vercauteren, D. P. *J. Phys. Chem. B* **1998**, *102*, 6507.
(8) van Tassel, P. R.; Somers, S. A.; Davis, H. T.; McCormick, A. V. *Chem. Eng. Sci.* **1994**, *49*, 2979.
(9) Beenakker, J. J. M.; Kuscer, I. *Zeolites* **1996**, *17*, 346.
(10) Kuscer, I.; Beenakker, J. J. M. *J. Stat. Physics* **1997**, *87*, 1083.
(11) Saravanan, C.; Jousse, F.; Auerbach, S. M. *Phys. Rev. Lett.* **1998**, *80*, 5754.
(12) Saravanan, C.; Auerbach, S. M. *J. Chem. Phys.* **1998**, *109*, 8755.
(13) Auerbach, S. M.; Metiu, H. I. *J. Chem. Phys.* **1996**, *105*, 3753.
(14) Auerbach, S. M.; Metiu, H. I. *J. Chem. Phys.* **1997**, *106*, 2893.
(15) Auerbach, S. M. *J. Chem. Phys.* **1997**, *106*, 7810.
(16) Saravanan, C.; Auerbach, S. M. *J. Chem. Phys.* **1997**, *107*, 8120.
(17) Saravanan, C.; Auerbach, S. M. *J. Chem. Phys.* **1997**, *107*, 8132.
(18) Saravanan, C.; Jousse, F.; Auerbach, S. M. *J. Chem. Phys.* **1998**, *108*, 2162.
(19) Blöchl, P. E.; van de Walle, C. G.; Pantelides, S. T. *Phys. Rev. Lett.* **1990**, *64*, 1401.
(20) Barthomeuf, D.; Ha, B.-H. *J. Chem. Soc., Faraday Trans. 1* **1973**, *12*, 2147.
(21) Barthomeuf, D.; Ha, B.-H. *J. Chem. Soc., Faraday Trans. 1* **1973**, *12*, 2158.
(22) Datka, J. *J. Chem. Soc., Faraday Trans. 1* **1981**, *77*, 511.
(23) Fitch, A. N.; Jobic, H.; Renouprez, A. *J. Phys. Chem.* **1986**, *90*, 1311.
(24) Burmeister, R.; Schwarz, H.; Boddenberg, B. *Ber. Bunsen-Ges. Phys. Chem.* **1989**, *93*, 1309.
(25) Liu, S.-B.; Ma, L.-J.; Lin, M.-W.; Wu, J.-F.; Chen, T.-L. *J. Phys. Chem.* **1992**, *96*, 8120.
(26) Pearson, J. G.; Chmelka, B. F.; Shykind, D. N.; Pines, A. *J. Phys. Chem.* **1992**, *96*, 8517.
(27) Su, B.-L. In *Zeolites: A Refined Tool for Designing Catalytic Sites*; Bonneviot, L., Kaliaguine, S., Eds.; Elsevier: Amsterdam, 1995; pp 303–310.
(28) Su, B.-L. *J. Chem. Soc., Faraday Trans.* **1997**, *93*, 1449.
(29) Sousa-Gonçalves, J. A.; Portsmouth, R. L.; Alexander, P.; Gladden, L. F. *J. Phys. Chem.* **1995**, *99*, 3317.
(30) Su, B.-L.; Barthomeuf, D. *J. Catal.* **1993**, *139*, 81.
(31) Demontis, P.; Yashonath, S.; Klein, M. L. *J. Phys. Chem.* **1989**, *93*, 5016.
(32) Uytterhoeven, L.; Dompas, D.; Mortier, W. J. *J. Chem. Soc., Faraday Trans.* **1992**, *88*, 2753.
(33) O'Malley, P. J.; Braithwaite, C. J. *Zeolites* **1995**, *15*, 198.
(34) Jousse, F.; Auerbach, S. M. *J. Chem. Phys.* **1997**, *107*, 9629.
(35) Klein, H.; Fuess, H.; Schrimpf, G. *J. Phys. Chem.* **1996**, *100*, 11101.
(36) Mosell, T.; Schrimpf, G.; Brickmann, J. *J. Phys. Chem. B* **1997**, *101*, 9476.
(37) Mosell, T.; Schrimpf, G.; Brickmann, J. *J. Phys. Chem. B* **1997**, *101*, 9485.
(38) Vitale, G.; Mellot, C. F.; Bull, L. M.; Cheetham, A. K. *J. Phys. Chem. B* **1997**, *101*, 4559.
(39) Vitale, G.; Bull, L. M.; Powell, B. M.; Cheetham, A. K. *J. Chem. Soc., Chem. Commun.* **1995**, *22*, 2253.

(40) Su, B.-L.; Manoli, J.-M.; Potvin, C.; Barthomeuf, D. *J. Chem. Soc., Faraday Trans*. **1993**, *89*, 857.

(41) Bull, L. M.; Cheetham, A. K.; Powell, B. M.; Ripmeester, J. A.; Ratcliffe, C. I. *J. Am. Chem. Soc*. **1995**, *117*, 4328.

(42) Kahn, R.; Mouche, E.; Cohen de Lara, E. *J. Chem. Soc., Faraday Trans*. **1990**, *86*, 1905.

(43) Demontis, P.; Fois, E. S.; Suffritti, G. B.; Quartieri, S. *J. Phys. Chem*. **1990**, *94*, 4329.

(44) Smirnov, K. S. *Chem. Phys. Lett*. **1994**, *229*, 250.

(45) Fritzsche, S.; Wolfsberg, M.; Haberlandt, R.; Demontis, P.; Suffritti, G. P.; Tilocca, A. *Chem. Phys. Lett*. **1998**, *296*, 253.

(46) Bouyermaouen, A.; Bellemans, A. *J. Chem. Phys*. **1998**, *108*, 2170.

(47) Demontis, P.; Suffritti, G. B. *Chem. Rev*. **1997**, *97*, 2845.

(48) Dobbs, K. D.; Doren, D. J. *J. Chem. Phys*. **1992**, *97*, 3722.

(49) Jacobsen, J.; Jacobsen, K. W.; Sethna, J. P. *Phys. Rev. Lett*. **1997**, *79*, 2843.

(50) Linderoth, T. R.; Horch, S.; Lægsgaard, E.; Stensgaard, I.; Besenbacher, F. *Phys. Rev. Lett*. **1997**, *78*, 4978.

(51) Allen, M. P.; Tildesley, D. J. *Computer Simulations of Liquids*; Clarendon Press: Oxford, 1987.

(52) Voter, A. F.; Doll, J. D. *J. Chem. Phys*. **1985**, *82*, 80.

(53) Chandler, D. *J. Chem. Phys*. **1978**, *68*, 2959.

(54) Voter, A. F. *J. Chem. Phys*. **1984**, *80*, 1890.

(55) Krause, K.; Geidel, E.; Kindler, J.; Förster, H.; Smirnov, K. S. *Vib. Spectrosc*. **1996**, *12*, 45.

(56) Jobic, H.; Fitch, A. N. In *Studies in Surface Science and Catalysis*; Chon, H., Ihm, S.-K., Uh, Y. S., Eds.; Vol. 105, pp 559−566, 1997.

(57) Schrimpf, G.; Schlenkrich, M.; Brickmann, J.; Bopp, P. *J. Phys. Chem*. **1992**, *96*, 7404.

(58) Chandler, D. *Introduction to Modern Statistical Mechanics*; Oxford University Press: New York, 1987.

(59) Frenkel, D.; Smit, B. *Understanding Molecular Simulations*; Academic Press: San Diego, 1996.

(60) Henson, N. J.; Auerbach, S. M. *DIZZY Computational Chemistry Program*; 1994−1998.